Chapter7

Theoretical study on Cobalt substituted Phthalocyanine for dye sensitizer solar cells

7.1 Introduction

To determine how the bluish CoPc (Fig. 7.1) is coupled to the surface, it is important to know the differences to free CoPc. First experimental results were obtained for the two crystalline phases α- and β-CoPc, solutions of CoPc and compounds of CoPc. More recently, experimentalists focused on multi-, mono- and submono-layers on different surfaces. Numerous articles deal with CoPc also from a theoretical point of view.

7.2 Structure

The distance to the next periodic repeated molecule was more than 7 Å. That the influence of the neighboring molecule is negligible small was verified by calculations with increasing distances between the molecules up to 20 Å.

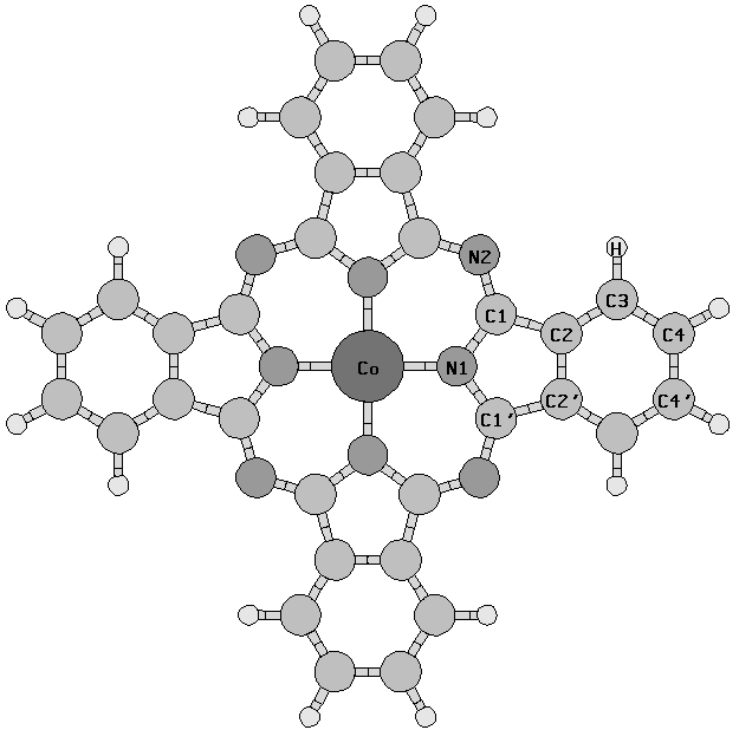

Figure 7.1 Cobalt phthalocyanine.

The optimized molecular structure of CoPc is illustrated in Fig. 7.1, where the central cobalt is bonded to four nitrogen. The overall symmetry is D_{4h}. The optimized bond length and angles are collected in Table 4.1 along with their experimental values. The computations of the dye Cobalt substituted phthalocyanine were done using DFT with Gaussian03 package. The DFT was treated according to Becke's three parameter gradient-corrected exchange potential and the Lee-Yang-Parr gradient-corrected correlation potential (B3LYP), and all calculations were performed without any symmetry constraints by using polarized split-valence 6-311++G(d,p) basis

sets. These calculations were done using CIS-DFT with the 6-311++G(d,p) basis sets and exchange-correlation functional in vacuum and the non-equilibrium version of the polarizable continuum model (PCM) was adopted for calculating the solvent effects.

Table 7.1 Calculated structural parameters of CoPc. Atom labels from Fig. 7.1.

Parameters	B3LYP/6-311++G(d-p)
Bond length	
Co3-N4	1.9134
Co3-N5	1.9261
N4-C12	1.4253
N4-C13	1.4714
N5-C14	1.4338
N5-C15	1.4237
N6-C12	1.3191
N6-C24	1.3854
N7-C13	1.3191
N7-C25	1.3854
N8-C14	1.38
N8-C26	1.3056
N9-C15	1.3798
N9-C27	1.309
N10-C24	1.3446
N10-C27	1.4336

N11-C25	1.3445
N11-C26	1.4336
C12-C16	1.4975
C13-C17	1.4975
C14-C18	1.4462
C15-C19	1.4463
C16-C17	1.418
C16-C20	1.3888
C17-C21	1.3808
C18-C19	1.4295
C18-C22	1.4076
C19-C23	1.4076
C20-C32	1.4063
C20-C44	1.1001
C21-C33	1.4063
C21-C45	1.1001
C22-C34	1.3782
C22-C46	1.0992
C23-C35	1.3782
C23-H47	1.1092
C24-C28	1.4899
C25-C29	1.4899
C26-C30	1.4896
C27-C31	1.4895
C28-C31	1.4369
C28-C36	1.3792
C29-C30	1.4369

C29-C37	1.3792
C30-C38	1.379
C31-C39	1.379
C32-C33	1.3918
C32-C48	1.1011
C33-C49	1.1011
C34-C35	1.4188
C34-H50	1.1003
C35-H51	1.1603
C36-C40	1.4053
C36-H52	1.0997
C37-C41	1.4054
C37-H53	1.0997
C38-C42	1.4059
C38-H54	1.1297
C39-C43	1.4058
C39-H55	1.0997
C40-C43	1.3918
C40-H56	1.1006
C41-C42	1.3917
C41-H57	1.1006
C42-H58	1.1011
C43-H59	1.1011
Bond Angle (in degree)	
Cl1- Co3-Cl2	89.8427
Cl1- Co3-N4	101.0388
Cl1- Co3-N5	103.4841

Cl2- Co3-N4	100.9817
Cl2- Co3-N5	103.4634
N4- Co3-N5	145.1404
Co3-N4-C12	126.4465
Co3-N4-C13	126.4817
12-N4-C13	105.7328
Co3-N5-C14	125.8811
Co3-N5-C15	125.8447
14-N5-C15	105.9424
C12-N6-C24	120.0999
C13-N7-C25	120.0967
C14-N8-C26	121.6489
C15-N9-C27	121.6532
C24-N10-C27	109.1345
C25-N11-C26	109.1291
N4-C12-N6	132.4084
N4-C12-C16	108.3545
N6-C12-C16	118.8447
N4-C13-N7	132.4066
N4-C13-C17	108.3563
N7-C13-C17	118.8436
N5-C14-N8	131.3261
N5-C14-C18	109.4315
N8-C14-C18	118.6852
N5-C15-N9	131.3296
N5-C15-C19	109.4197
N9-C15-C19	118.6902

C12-C16-C17	106.9966
C12-C16-C20	131.7473
C17-C16-C20	121.2546
C13-C17-C16	106.9974
C13-C17-C21	131.7464
C16-C17-C21	121.2547
C14-C18-C19	106.9651
C14-C18-C22	132.5737
C19-C18-C22	120.4304
C15-C19-C18	106.9678
C15-C19-C23	132.573
C18-C19-C23	120.4281
C16-C20-C32	117.4978
C16-C20-H44	121.4636
C32-C20-H44	121.0383
C17-C21-C33	117.4978
C17-C21-H45	121.4634
C33-C21-H45	121.0385
C18-C22-C34	118.159
C18-C22-H46	119.9947
C34-C22-H46	121.8448
C19-C23-C35	118.1594
C19-C23-C47	119.9944
C35-C23-H47	121.8447
N6-C24-N10	124.1241
N6-C24-C28	125.284
N10-C24-C28	110.3777

N7-C25-N11	124.1306
N7-C25-C29	125.2697
N11-C25-C29	110.3832
N8-C26-N11	124.1987
N8-C26-C30	127.9405
N11-C26-C30	107.4282
M9-C27-N10	124.1885
N9-C27-C31	127.9556
N10-C27-C31	107.4274
C24-C28-C31	105.8282
C24-C28-C36	133.1619
C31-C28-C36	121.0075
C25-C29-C30	105.8266
C25-C29-C37	133.163
C30-C29-C37	121.0081
C26-C30-C29	106.4139
C26-C30-CC38	132.8466
C29-C30-C38)	120.7342
C27-C31-C28	106.4157
C27-C31-C39	132.8473
C28-C31-C39	120.7319
C20-C32-C33	121.2463
C20-C32-H48	118.9921
C33-C32-H48	119.7615
C21-C33-C32	121.2462
C21-C33-H49	118.9922
C32-C33-H49	119.7615

C22-C34-C35	121.4085
C22-C34-H50	120.0745
C35-C34-H50	118.5169
C23-C35-C34	121.4104
C23-C35-H51	120.0733
C34-C35-H51	118.5162
C28-C36-C40	117.8116
C28-C36-H52	121.311
C40-C36-H52	120.8772
C29-C37-C41	117.8105
C29-C37-H53	121.315
C41-C37-H53	120.8744
C30-C38-C42	117.8522
C30-C38-H54	121.2748
C42-C38-H54	120.8727
C31-C39-C43	117.8535
C31-C39-H55	121.2703
C43-C39-H55	120.8758
C36-C40-C43	121.2096
C36-C40-H56	119.0475
C43-C40-H56	119.7428
C37-C41-C42	121.2099
C37-C41-H57	119.0442
C42-C41-H57	119.7456
C38-C42-C41	121.3843
C38-C42-H58	118.948
C41-C42-H58	119.6675

C39-C43-C40	121.3851
C39-C43-H59	118.9506
C40-C43-H59	119.664
Dihedral Angles (in degree)	
Co3-N4-C12-N6	38.5803
Co3-N4-C12-C16	-148.9143
C13-N4-C12-N6	-154.0127
Co3-N4-C13-N7	-38.5958
Co3-N4-C13-C17	148.9097
C12-N4-C13-N7	154.003
Co3-N5-C14-N8	36.5896
Si3-N5-C14-C18	-152.3012
C15-N5-C14-N8	-160.0171
Co3-N5-C15-N9	-36.61
Co3-N5-C15-C19	152.3068
C14-N5-C15-N9	159.9889
C24-N6-C12-N4	-6.6387
C24-N6-C12-C16	-178.5138
C12-N6-C24-N10	0.3472
C12-N6-C24-C28	-173.8176
C25-N7-C13-N4	6.6459
C25-N7-C13-C17	178.5093
C13-N7-C25-N11	-0.3912
C13-N7-C25-C29	173.7418
C26-N8-14-N5	1.0106
C26-N8-14-18	-169.426
C14-N8-26-N11	-6.7518

C14-N8-C26-C30	-178.2339
C27-N9-C15-N5	-0.9469
C27-N9-C15-C19	169.4605
C15-N9-C27-N10	6.7385
C15-N9-C27-C31	178.2603
C27-N10-C24-N6	-165.8779
C27-N10-C24-C28	9.0429
C24-N10-C27-N9	163.9321
C24-N10-C27-C31	-9.0695
C26-N11-C25-N7	165.8419
C26-N11-C25-C29	-9.0502
C25-N11-C26-N8	-163.8797
C25-N11-C26-C30	9.0876
N4-C12-C16-C17	-11.5508
N4-C12-C16-C20	168.8992
N6-C12-C16-C17	162.1369
N4-C13-C17-C16	11.5483
N4-C13-C17-C21	-168.904
N7-C13-C17-C16	-162.1301
N5-C14-C18-C19	-6.9549
N5-C14-C18-C22	175.1235
N8-C14-C18-C19	165.4425
N5-C15-C19-C18	6.9611
N5-C15-C19-C23	-175.1267
N9-C15-C19-C18	-165.4142
C12-C16-C17-C13	0.002
C12-C16-C17-C21	-179.6032

C20-C16-C17-C13	179.6092
C12-C16-C20-C32	179.8999
C12-C16-C20-H44	-0.2868
C17-C16-C20-C32	0.4033
C13-C17-C21-C33	-179.8996
C13-C17-C21-H45	0.2782
C16-C17-C21-C33	-0.4056
C14-C18-C19-C15	-0.0049
C14-C18-C19-C23	-178.222
C22-C18-C19-C15	178.22
C14-C18-C22-C34	178.2073
C14-C18-C22-H46	-2.2223
C19-C18-C22-C34	0.5131
C15-C19-C23-C35	-178.2012
C15-C19-C23-H47	2.2248
C18-C19-C23-C35	-0.5172
C16-C20-C32-C33	-0.4089
C16-C20-C32-H48	179.5786
44-C20-C32-C33	179.7769
C17-C21-C33-C32	0.3999
C17-C21-C33-H49	-179.5651
45-C21-C33-C32	-179.777
C18-C22-C34-C35	-0.52
C18-C22-C34-H50	179.4012
D46-C22-C34-C35	179.918
C19-C23-C35-C34	0.5209
C19-C23-C35-H51	-179.402

47-C23-C35-C34	-179.9134
N6-C24-C28-C31	169.4453
N6-C24-C28-C36	-9.9719
N10-C24-C28-C31	-5.4037
N7-C25-C29-C30	-169.424
N7-C25-C29-C37	10.0077
N11-C25-C29-C30	5.3971
N8-C26-C30-C29	167.1051
N8-C26-C30-C38	-12.0309
N11-C26-C30-C29	-5.5176
N9-C27-C31-C28	-167.1609
N9-C27-C31-C39	11.993
N10-C27-C31-C28	5.4953
C24-C28-C31-C27	-0.3163
C24-C28-C31-3C9	-179.5946
C36-C28-C31-C27	179.1877
C24-C28-C36-C40	179.6244
C24-C28-C36-H52	-0.2383
C31-C28-C36-C40	0.2786
C25-C29-C30-C26	0.334
C25-C29-C30-C38	179.597
C37-C29-C30-C26	-179.1824
C25-C29-C37-C41	-179.643
C25-C29-C37-H53	0.2474
C30-C29-C37-C41	-0.2809
C26-C30-C38-C42	179.1981
C26-C30-C38-H54	-0.5755

C29-C30-C38-C42	0.1624
C27-C31-C39-C43	-179.2128
C27-C31-C39-H55	0.5794
C20-C32-C33-C21	0.0075
C20-C32-C33-H49	179.9723
H48-C32-C33-C21	-179.9799
C22-C34-C35-C23	0.0005
C22-C34-C35-H51	179.9244
H50-C34-C35-C23	-179.922
C28-C36-C40-C43	-0.2247
C28-C36-C40-H56	179.9089
H52-C36-C40-C43	179.6386
C29-C37-C41-C42	0.2439
C29-C37-C41-H57	-179.9237
H53-C37-C41-C42	-179.647
C30-C38-C42-C41	-0.2012
C30-C38-C42-H58	179.9608
H54-C38-C42-C41	179.5734
C31-C39-C43-C40	0.2127
C31-C39-C43-H59	-179.9827
H55-C39-C43-C40	-179.5804
C36-C40-C43-C39	-0.0218
C36-C40-C43-H59	-179.8251
H56-C40-C43-C39	179.8436
C37-C41-C42-C38	-0.0025
C37-C41-C42-H58	179.8344
H57-C41-C42-C38	-179.8338

If we use the crystal field theory to describe the electronic structure of CoPc, the quadratic planar coordination of the cobalt(II)-ion results in splitting of the degenerated d-orbitals as shown in Fig. 7.2. But since the cobalt-nitrogen distance (~ 1.9 Å Tab. 7.1) is similar to the sum of the covalent radius of N (0.70 Å) and Co (1.16 Å) a bonding between Co and N can't be excluded. Thus, molecular orbital theory has to be applied. Within this theory the ligands and the transition metal can form covalent bonds. Therefore, the splitting of the d-orbitals is not only due to the electrostatic influence of the ligands. The D_{4h} symmetry leads to a formation of the metal d-orbitals, as follows: $d_{x^2-y^2}$, d_{xz}/d_{yz} and d_{xy}, d_{z^2} (from lowest to highest energy). Additionally, we have to consider p-bonds, which will complicate the energy-level diagram even more.

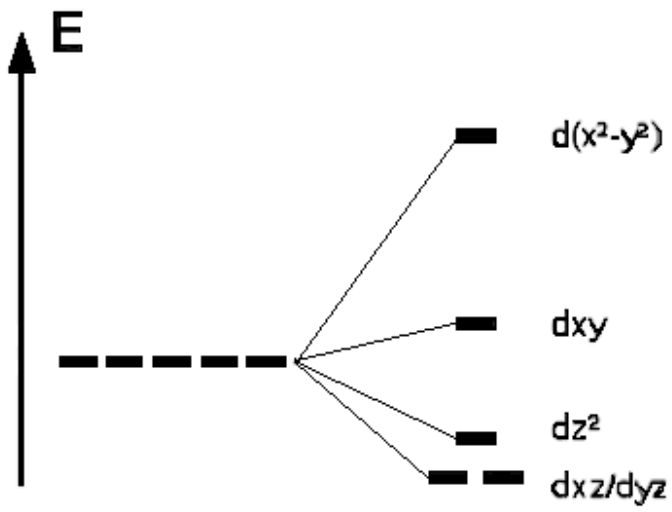

Figure 7.2 Crystal field splitting diagram for a quadratic planar coordination.

The B3LYP/6-311++G(d,p) result indicates hybridization between the cobalt d_{x2-y2} and nitrogen p_x/p_y as it can clearly be seen in Figs. 7.3 and 7.4 between -6 eV and -4 eV. Furthermore one can identify π-bonding between the cobalt d_{xz}/d_{yz} and the pz of nitrogen at about -3.33 eV and -1.66 eV. The DFT calculation yields d_{z^2} as the lowest unoccupied molecular orbital (LUMO) and d^*_{xz}/d^*_{yz} as highest occupied molecular orbital (HOMO).

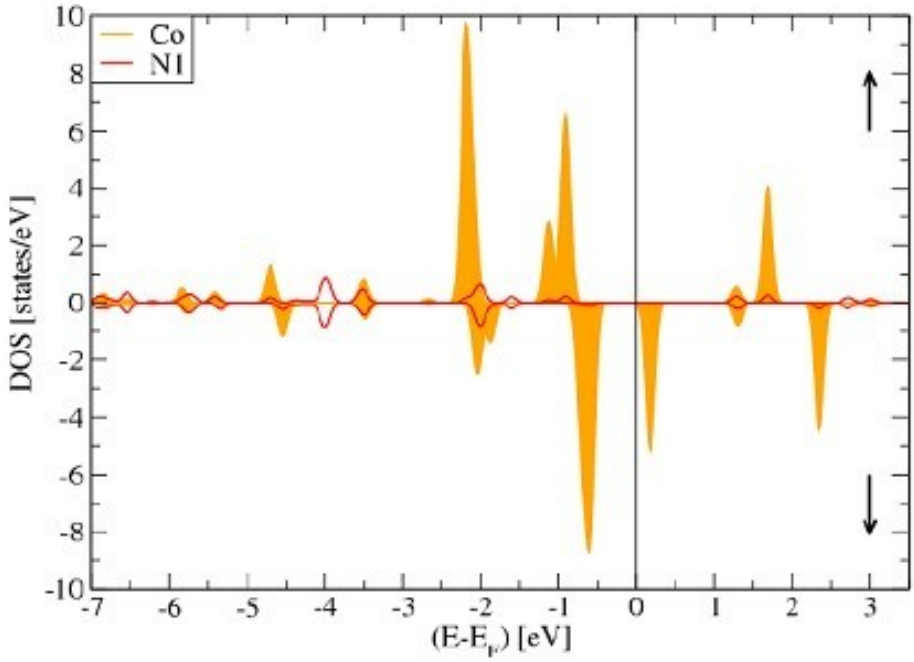

Figure 7.3 Spin resolved projected DOS of CoPc calculated with B3LYP/6-311++G(d,p). Orange is the DOS for the cobalt d-orbitals and the red line are the nitrogen N1 p-orbitals. Positive values of the DOS correspond to spin up and negative values to spin down.

Since CoPc belongs to the D_{4h} point group, the x- and y-direction are equal. Hence, the d_{xz}/d_{yz}-orbitals should be energetically degenerated. In Fig. 7.4 we observe two states with m = 1 – one at -3.33 eV and the second at -1.66 eV, both with the same portions of d_{xz} and d_{yz} (the states near EF and 1.7 eV are the corresponding anti-bonding states). The DFT code correctly recognizes the 16 symmetry operations of the point group, but it treats the two spin channels as different k-points. DFT uses a Gaussian broadening scheme of the electronic states, which my result in accidently broken symmetry.

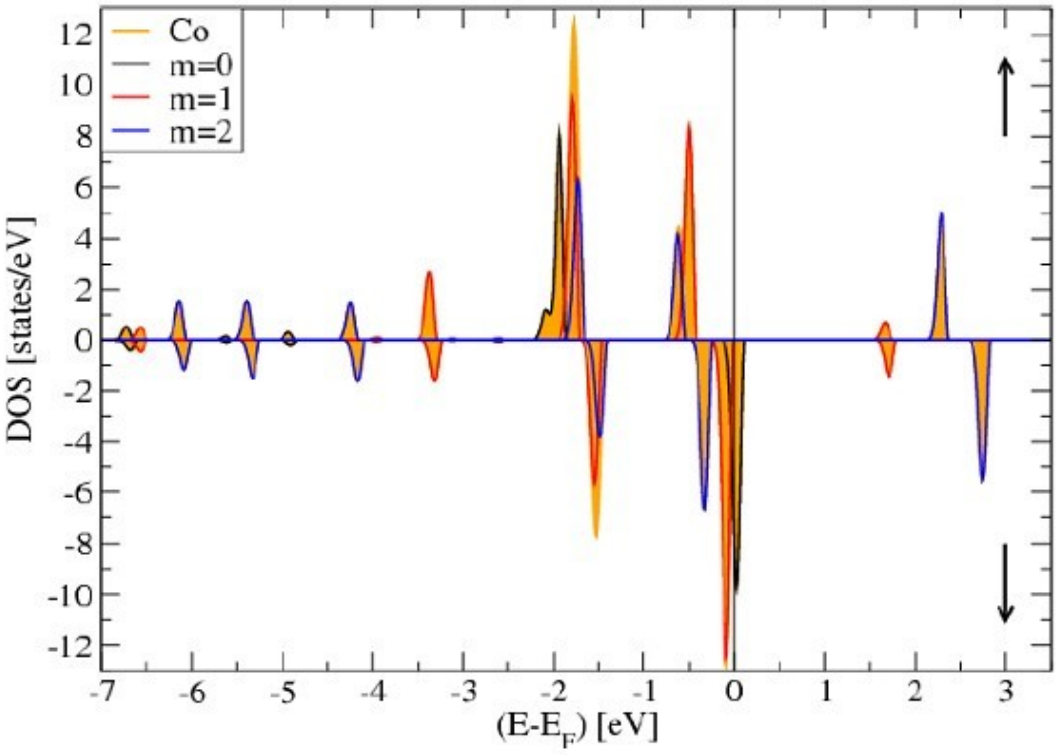

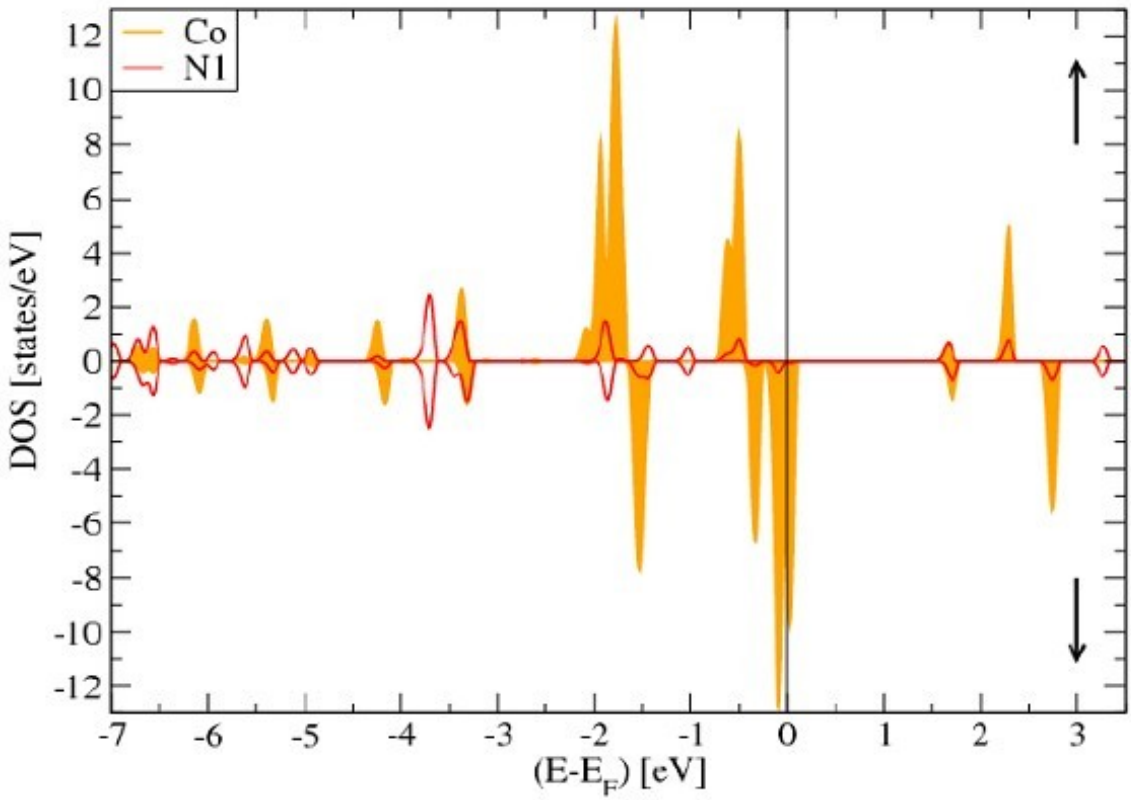

Figure 7.4 Spin resolved projected DOS of CoPc calculated with DFT using the B3LYP/6-311++G(d,p). In A the DOS of Co is shown. For clarity the d-contribution is split into different values of m, which deliver information on the d-states involved. In the second panel the DOS for the cobalt d-orbitals and the nitrogen N1 porbitals (Fig. 7.3) is given. Positive values of the DOS correspond to spin up and negative values to spin down.

7.3 HOMO-LUMO energy gap of Cobalt substituted Phthalocyanine dye sensitizer

The (HOMO) and (LUMO) are very important parameters for quantum chemistry. These orbitals are sometimes called the frontier orbitals, because they lie at the outermost boundaries of the electrons of the molecules.

Both the (HOMO) and (LUMO) are the main orbitals that take part in chemical stability. The difference of the energies of the HOMO and LUMO, the band gap serves as a measure of the excitability of the molecule, the smaller the energy, more easily it will be excited.

The HOMO–LUMO gap of the dye Cobalt substituted phthalocyanine in vacuum is 1.87 eV. While the calculated HOMO and LUMO energies of the bare $Ti_{38}O_{76}$ cluster as a model for nanocrystalline are -6.55 and -2.77 eV, respectively, resulting in a HOMO–LUMO gap of 3.78 eV, the lowest transition is reduced to 3.20 eV according to TD-DFT, and this value is slightly smaller than typical band gap of TiO_2 nanoparticles with nm size [1]. Furthermore, the HOMO, LUMO and HOMO–LUMO gap of $(TiO_2)_{60}$ clusters is -7.52, -2.97 and 4.55 eV (B3LYP/VDZ), respectively [2]. Taking into account of the cluster size effects and the calculated HOMO, LUMO, HOMO–LUMO gap of the dye Cobalt substituted phthalocyanine, $Ti_{38}O_{76}$

and $(TiO_2)_{60}$ clusters, we can find that the HOMO energies of these dyes fall within the TiO_2 gap.

The above data also reveal the interfacial electron transfer between semiconductor TiO_2 electrode and the dye sensitizer Cobalt substituted phthalocyanine is electron injection processes from excited dye to the semiconductor conduction band. This is a kind of typical interfacial electron transfer reaction.

In addition to the aggregation of the dye, electronic structure also affects photovoltaic performance significantly. In DSSCs, one of the most important features for a metal substituted organic dye is intramolecular charge transfer (ICT) from electron donating part to the electron accepting part. The electronic structures of HOMO-1, HOMO, LUMO and LUMO+1 of the cobalt substituted phthalocyanine dye are shown in Figure 7.5, and this dye has good electron-separated states.

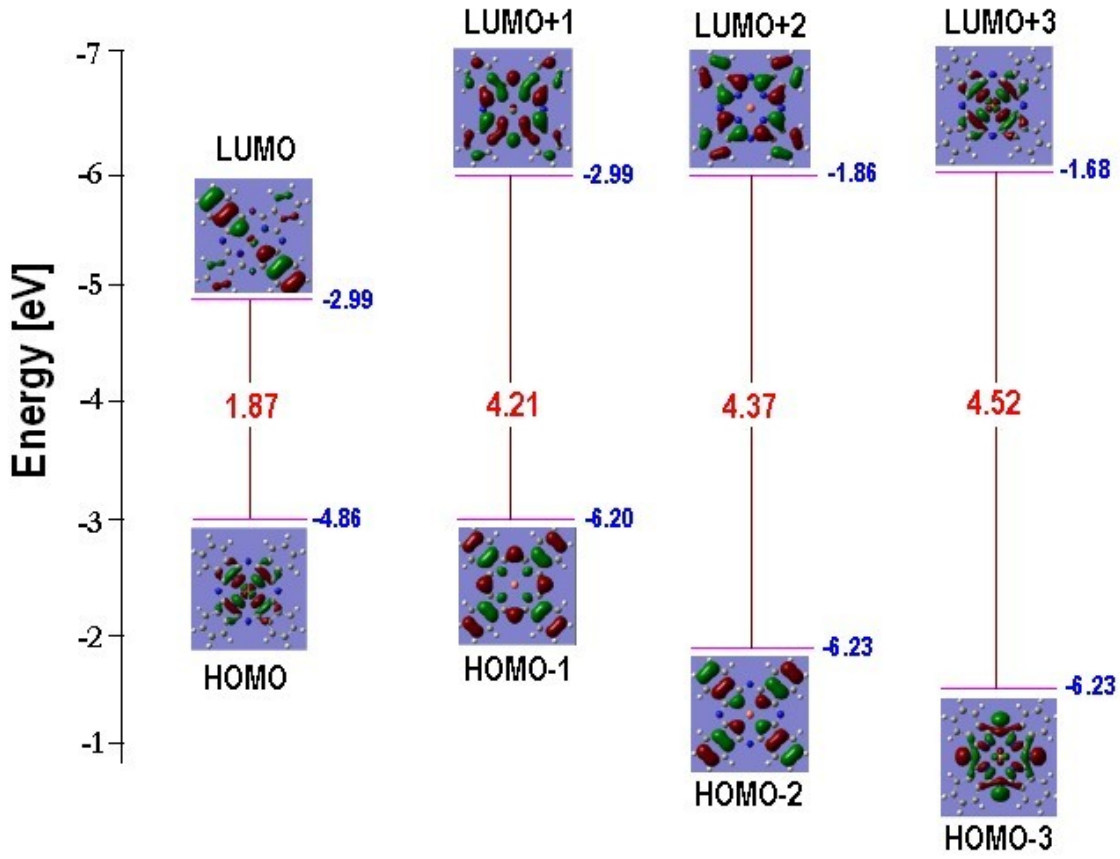

Figure 7.5 Molecular orbital spatial distribution for Cobalt substituted Phthalocyanine.

The electron densities of HOMO of cobalt substituted phthalocyanine is localized on the donor and the bridge, whereas the electron density of LUMO is mainly localized on the bridge and acceptor units (mostly in the anchoring group), so the electronic transitions of cobalt substituted phthalocyanine from HOMO to LUMO could lead to intramolecular charge transfer from the donor units to the anchoring groups through the conjugated bridge. Therefore, when the dyes are anchored on the surface

of TiO_2, the LUMO centered on the anchoring moiety should enhance the orbital overlap with the titanium 3d orbital and subsequently favor the electron injection to the conduction band of TiO_2.

Corresponding data of HOMO, LUMO, and HOMO-LUMO gaps are showned in figure 7.5. We know that LUMO energy levels of the three dyes are much higher than that of TiO_2 conduction band edge (ca -4.0 eV) [3]. Thus, molecules in excited states of cobalt substituted phthalocyanine have a strong ability to inject electrons into TiO_2 electrodes. The HOMO of the dye is lower than that of I^-/I^-_3 (ca -4.8 eV) [4], therefore, these molecules that lose electrons could be restored by getting electrons from electrolyte. The order of the LUMO energy gap is cobalt substituted phthalocyanine (-2.99 eV), thus, the driving forces for electron injection from molecular excitation state of the dyes to TiO_2 electrode. The order of the HOMO-LUMO gap is cobalt substituted phthalocyanine (1.87 eV). With the HOMO-LUMO gap decrease, more photons at the longer-wavelength side would be absorbed to excite the electrons into the unoccupied molecular orbital, which increases the short circuit current density and further enhances the conversion efficiency of the corresponding solar cell.

7.4 UV-Vis spectra of Cobalt substituted Phthalocyanine

The UV-Vis spectra of Cobalt substituted phthalocyanine were measured in acetonitrile solution, and it is found that the absorption bands centered at

676 nm in UV region. Electronic absorption spectra of Cobalt substituted phthlocyanine in solvent were performed using CIS-DFT(B3LYP)/6-311++G(d,p) calculations, and the results are shown in Fig. 7.6. It is observed that, for Cobalt substituted phthalocyanine, the absorption in the visible region is much weaker than that in the UV region.

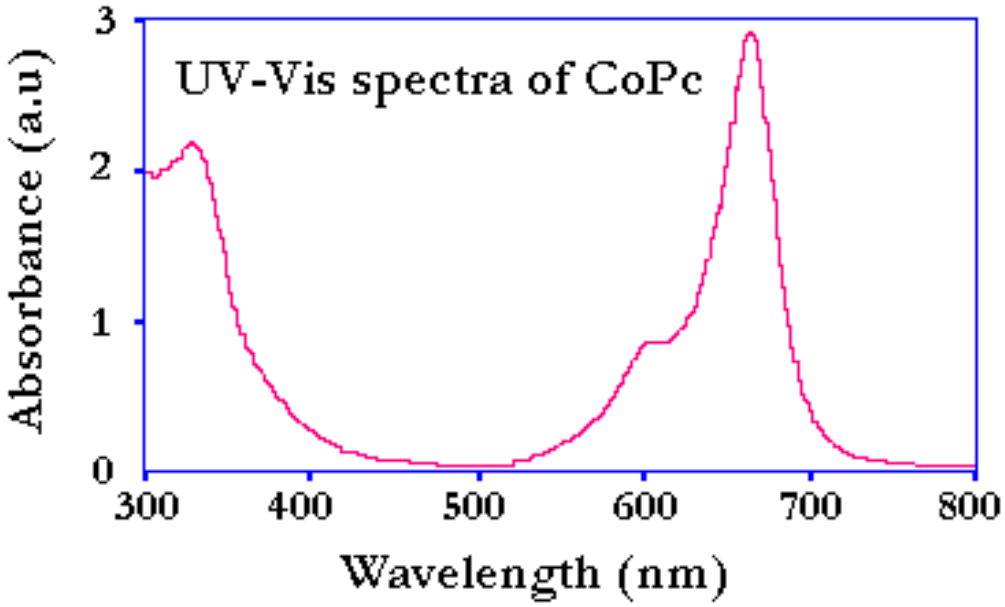

Figure 7.6 UV/Vis electronic absorption spectra of Cobalt substituted phthalocyanine in acetonitrile solvent.

The results of CIS-DFT have an appreciable red-shift in experimental results, and the degree of red-shift in calculated CIS-DFT is more significant than that in experimental results (In experimental data is not included). The discrepancy between experimental and CIS-DFT calculations may result

from two aspects. The first aspect is smaller gap of materials which induces smaller excited energies. The other is solvent effects. Experimental measurements of electronic absorptions are usually performed in solution. Solvent, especially polar solvent, could affect the geometry and electronic structure as well as the properties of molecules through the long-range interaction between solute molecule and solvent molecule. For these reasons it is more difficult to make the CIS-DFT calculation in vacuum is consistent with quantitatively. Though the discrepancy exists, the CIS-DFT calculations in solvent are capable of describing the spectral features of Cobalt substituted phthalocyanine because of the agreement of line shape and relative strength as compared with the experimental and calculated values.

References

[1] M. K. Nazeeruddin, F. De Angelis, S. Fantacci, A. Selloni, G. Viscardi, P. Liska, S.Ito, B. Takeru, M. Gratzel, J. Am. Chem. Soc. 2005, 127, 16835.

[2] M. J. Lundqvist, M. Nilsing, P. Persson, S. Lunell, Int. J. Quantum Chem. 2006, 106, 3214.

[3] J.B. Asbury, Y.Q. Wang, E. Hao, H. Ghosh, T. Lian, Res. Chem. Intermed. 2001, 27, 393.

[4] D. Cahen, G. Hodes, M. Grätzel, J.F.Guillermoles, I. Riess, J. Phys. Chem. B 2000, 104, 2053.